

HYDROXYAPATITE NANOPARTICLES ALLEVIATE THE ADVERSE HEALTH PROBLEMES OF BISPHENOL A

**Sara M. Ebrahim⁽¹⁾; Mohamed Mokhtar⁽²⁾; Hala M. Al- Desouky⁽³⁾
and Germiné M. Hamdy⁽³⁾**

1) Environmental basic sciences, faculty of graduate studies and research, Egypt 2) Chemical Engineering Department, Military Technical College, Egypt 3) Biochemistry Department, Faculty of Science, Ain Shams University, Egypt

ABSTRACT

Bisphenol A (BPA) is one of the most detrimental pollutants in environment. Inside the body, it is metabolized by the liver and hence triggers liver injury. Hydroxyapatite nanoparticles (HANPs) are selected in the current study as a safe way to adsorb the BPA and hence eliminate its toxic impacts *in vivo*.

HANPs formula was prepared by sol-gel techniques; characterization was confirmed by XRD, FTIR, morphology and thermal stability. *In vivo* study was conducted on Forty male rats which were equally divided into 4 groups. The negative control received 10%DMSO solution, HANPs group were ingested with 1g/ kg b.wt./day of HANPs, BPA group received 100 mg BPA/ kg b.w.t/ day, and the BPA+HANPs group were treated with 1 g HANPs/100mg BPA/ kg b.w.t/ day. The doses were given daily for six consecutive weeks orally. Blood samples were collected; serum was separated and used for determination of selected liver enzymes and lipid profile parameters.

ALT and AST levels were significantly increased with concomitant decrease in the total protein and albumin levels in the BPA group, compared to the control one. Cholesterol, Triglycerides and LDL-Cholesterol levels

were also increased with concomitant decrease in the HDL-Cholesterol in the BPA group. On the other hand, BPA+HANPs group exhibited amelioration in the lipid profile parameters, as compared to the BPA one.

In conclusion, HANPs can be considered as a promising and effective biomaterial that can alleviate liver injury induced by exposure to the BPA pollutant.

Key words: Bisphenol A, health problems, liver enzymes, lipid profile, Hydroxyapatite nanoparticles.

INTRODUCTION

Water pollution has emerged as one of the most serious threats to humans and other organisms. Water bottles, inner coatings for canned goods, dental sealants, and other products all include bisphenol A (2, 2-bis [4-hydroxyphenyl] propane, or BPA), the phenol which is utilized in the manufacture of polycarbonate plastic products (Hernandez- Rodriguez *et al.*, 2007). BPA was found in food and water as a result of the use of plastic items (Michalowicz, 2014). It is released into water or foods when these plastics are heated or exposed to ultraviolet light, and when people come into contact with it (Noureddine *et al.*, 2018). Unfortunately, BPA cannot be completely eliminated by traditional treatment procedures (Braga *et al.*, 2005), which allows it to reenter the water, marine and soil environments (Rochester, 2013; Xu *et al.*, 2014).

In Egypt, it was discovered that BPA was present in large quantities in a variety of water sources. Radwan *et al.* (2020), who looked into the prevalence and distribution of BPA in 23 Egyptian governorates, reported that

33.0% of the water sources tested positive for BPA, which was associated with effluent discharge from wastewater treatment or partially treated factory wastewater (Fan *et al.*; 2013). BPA is present in drinking water from the Dakahlia source at a rate of 14.5%, according to sampling results. Due to industrial discharge, Alexandria, the governorate with the greatest source water in Egypt, had the highest BPA contents, with values of 2800, 22,300, and 85,500 ng/L (Radwan *et al.*, 2020).

BPA exposure occurs primarily through ingestion, skin penetration, and inhalation (Rubin, 2011). BPA affects numerous organs, such as the liver, kidney, lungs, spleen, and pancreas (Petteri, 2002). BPA exposure is associated with a variety of health problems including type 2 diabetes, dyslipidemia, hypertension, and liver damage (Alonso-Magdalena *et al.*, 2006). Additionally, children who have been exposed to BPA as an environmental toxin are more likely to develop autism spectrum disorders (Ye *et al.*, 2017). The U.S. Environmental Protection Agency reported that the reference dose of BPA is 50 µg/kg/day but the European Food Safety Authority (EFSA) reduced this dose to 4 µg/kg/day (Corrales *et al.*; 2015). As BPA is primarily metabolized by the liver, the conjugation takes place in the liver by glucuronidation *via* the glucuronyl transferase enzyme and is then excreted in the intestine and urine (Lindholm *et al.*, 2003; Hanioka *et al.*, 2008). Increased BPA levels in humans have been linked with liver injury, as evidenced by alteration in serum levels of liver enzymes; ALT and AST

(Lang *et al.*, 2008; Mourad & Khadrawy, 2012) as well as prompt oxidative stress in vital organs for instance kidney, liver and testis (Bindhumol *et al.*, 2003; Chitra *et al.*, 2003; Kabuto *et al.*, 2004; Mourad & Khadrawy, 2012). The Liver may be more sensitive to BPA exposure than other organs (Moon *et al.*, 2012). BPA activates Kupffer cells in the liver, causing the production of several cytokines, which is evidence for liver inflammation and progress of liver diseases (Kopf *et al.*, 2010; Wu *et al.*, 2010). So, the development of an effective and safe method for BPA removal is urgently needed.

Nowadays, there is a great attention in using nanomaterials to remove the toxic and destructive substances from wastewater (Kuhn, 2022). These nanomaterials had a large surface area and unique properties than larger ones (Gupta *et al.*, 2011). Hydroxyapatite (HAP) is the most stable calcium phosphate salt at room temperature with a pH range of 4 to 12 (Surmenev *et al.*, 2014; Prakasam *et al.*, 2015) and was early applied to study biomineralization phenomena (Dorozhkin, 2012). It is a safe chemical that is similar to the normal bone tissue composition, as well as a form of calcium phosphate with the chemical formula $\text{Ca}_{10}(\text{PO}_4)_6(\text{OH})_2$. Importantly, HANPs has become of great interest to enter *in vitro* and *in vivo* research, surgery, and medical applications (Descamps *et al.*, 2009; Fihri *et al.*, 2017).

HANPs were successfully prepared by different methods, including solid state reaction, hydrothermal, sol-gel, plasma technique and layer hydrolysis (Hsieh *et al.*, 2001).

In this study, we prepared the HANPs as a unique BPA elimination procedure using the sol-gel method. Further *in vivo* testing was conducted to determine the effectiveness and capability of these HANPs in removing BPA toxicity.

MATERIALS AND METHODS

1. MATERIALS:

Calcium nitrate tetrahydrate ($\text{Ca}(\text{NO}_3)_2 \cdot 4\text{H}_2\text{O}$), Purity > 98%, and Bisphenol A $\text{Ca}_{10}(\text{PO}_4)_6(\text{OH})_2$ (purity $\geq 99\%$), were purchased from Sigma-Aldrich, St. Louis, MO, USA. Phosphorous Pentoxide (P_2O_5) of purity 98% and absolute Ethyl alcohol were purchased from Spectrum, USA.

2. METHODS:

2.1. Preparation of hydroxyapatite nanoparticles (HANPs) powder

The synthesis of HANPs is performed using the sol-gel method according to Fathi *et al.*, (2008). Briefly, Calcium nitrate tetrahydrate and phosphorous pentoxides which are used as precursor are dissolved in absolute ethanol and mixed well. Then, a gelation process was conducted on the mixture for 1 hour, following by an aging step for another 1 hour, and the gel was dried at 100°C . Finally, a sintering process was performed at temperature varied from 600°C to 800°C .

3. Characterization of the prepared HANPs

In order to compare between the prepared HANPs in the current study and the previous ones, the characterization was performed as illustrated below

on the prepared particles; including the morphology and the particle size distribution, crystallinity and phase composition, functional groups and thermal stability.

3.1. Morphology and particle size distribution of HANPs: The morphology of HANPs and their particles size were examined using scanning electron microscope ZEISS at different scale varying from 1 μ m to 100 μ m.

3.2. Crystallinity and phase composition of HANPs: X-ray Diffraction (XRD) was carried out to identify the crystallographic structural of the sample using XTRA Powder diffractometer by thermo Scientific. Operated at X-ray tube 40.0 (kV) voltage, 30.0 (mA) current) recorded peaks in the 2 θ range from 4.0°-90.0°. Scan mode is continuous with 8.0000 °/min speed at step size 0.02° and preset time 0.15 sec.

3.3. Identification of functional group of HANPs: Fourier Transform Infrared Spectrometer (FT/IR-4100) was used for the identification of the functional group in the prepared HANPs. The number of scans was adjusted at 300, the spectrum was scanned from 400-4000 cm⁻¹ with 8 cm⁻¹ resolution, and the vertical axis represents the single %Transmittance background.

3.4. Thermal stability: In order to evaluate the thermal stability of the prepared HANPs, an amount of 2 mg from the sample was placed at High-temperature Platinum crucible, then the crucible was transferred to the thermal gravimetric (TG) sample holder assembly which had been set at room temperature (25°C) and all other thermal measurements were carried out at

temperature range from 50°C to 850°C, with heating rate of 10°C/min. All thermal decomposition process was carried out in an inert atmosphere (N₂, 40 ml/min⁻¹) by using TGA55 (TA Instruments, USA) to record the thermal decomposition for HANPs.

4. *In vivo* study

4.1. Animals and experimental protocol: A total of Forty adult male Wister rats (175 to 200g) were maintained under standard laboratory conditions; temperature 22±2°C, and 12h-12h light/dark cycle with proper human care. They were acclimatized for a week before starting the experiments and allowed to free access of food and water. The experimental protocol was approved by the local institutional animal ethics committee of Ain Shams University. The rats were randomly divided into 4 equal groups (n=10). The experiment was designed to unify the conditions as BPA was dissolved in 10% DMSO, so the negative control was designed to receive the same used vehicle (10% DMSO). In our previous studies, we confirm the biosafety of the use of this DMSO concentration on rats as 10% DMSO exhibited no harm effects on the used experimental animals. Group I; served as negative control: animals received 10% DMSO solution. Group II; HANPs: rats ingested with 1g/ kg b.wt./day of HANPs, Group III; BPA: animals received 100 mg/kg/bwt./day of BPA dissolved in 10% DMSO. Group IV; HANPs + BPA: animals were ingested with 1g HANPs/100 mg BPA/ kg b.w.t/ day. Ingestion was taken orally by gastric gavage for 6 consecutive weeks in all groups.

4.2. Liver function tests: Serum alanine transaminase (ALT, EC: 2.6.1.2), and aspartate transaminase (AST, EC: 2.6.1.1) activities were estimated by using commercial kits (SPECTRUM diagnostic kits, Egypt), according to the method of Reitman and Frankel (1957). Total protein and albumin contents were also determined in serum according to the method of Lowry *et al.*, (1951).

4.3. Lipid profile: The levels of serum total cholesterol; T-Ch (Allain *et al.*, 1974), triglycerides; TGs (Fossati and Prencipe, 1982), high-density lipoprotein-cholesterol; HDL-cholesterol (Finley *et al.*, 1978) were determined colorimetrically using the commercial kits (SPINREACT diagnostic kit). LDL-Cholesterol was calculated using the following equation:
$$\text{LDL} = \text{Total cholesterol} - (\text{triglycerides}/5) \times \text{HDL-cholesterol}$$

5 Statistical analysis

Statistical analysis was conducted using the SPSS program, version 23.0 for Windows (SPSS® Chicago, IL, USA). Data were expressed as mean values \pm SD. Results were statistically significant as $p \leq 0.05$.

RESULTS

1. Characterization of HANPs

1.1. Morphology and size: The surface morphology of the hydroxyapatite powder was investigated by Scanning Electron Microscope (SEM). The results from SEM characterization show that HANPs are very fine particles of irregular shape, which clumped in form of clusters. These clusters contain pores of different sizes. The observed fine particles are in the nano scale, while their clusters are in micro scale (Figure 1).

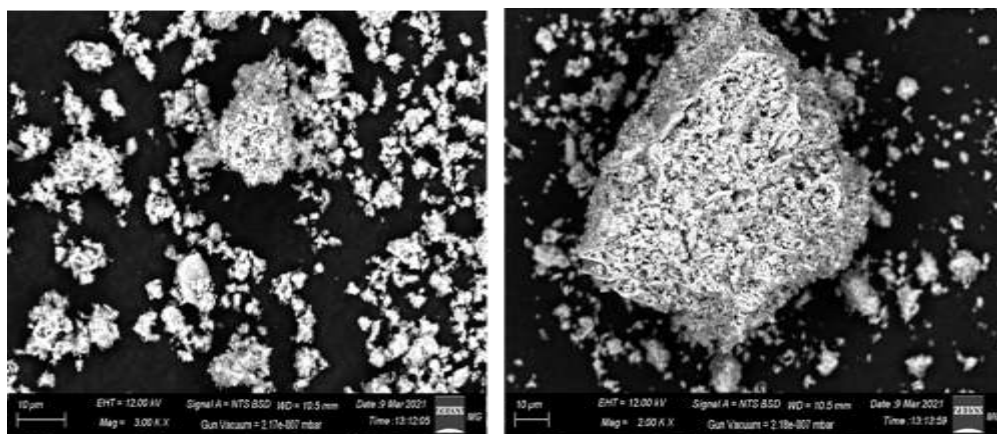


Figure 1. Scanning electron microscope HANPs

1.2. Crystallinity and phase description of HANPs: Figure 2 depicts the X-ray diffraction (XRD) pattern of the synthesized HANPs, which shows discrete Sharpe peaks at 2θ angle of 3 strong peaks of 32.04, 33.177 and 32.44 , and also at 26.095, 46.93, 49.742 with d- spacing values of 2.79 Å, 2.69 Å and 2.75 Å 3.41 Å, 1.93 Å, 1.831 Å, respectively. Using the following Scherrer equation, the calculated grain size of HANPs was 65 nm.

$$D = k\lambda / \beta \cos \theta$$

k is a constant related to crystallite shape that is usually taken as 0.9, λ represent the X-ray wavelength in nanometers (nm), β is the peak width of the diffraction peak profile at half its maximum height in radians (Mahabole *et al.*, 2005).

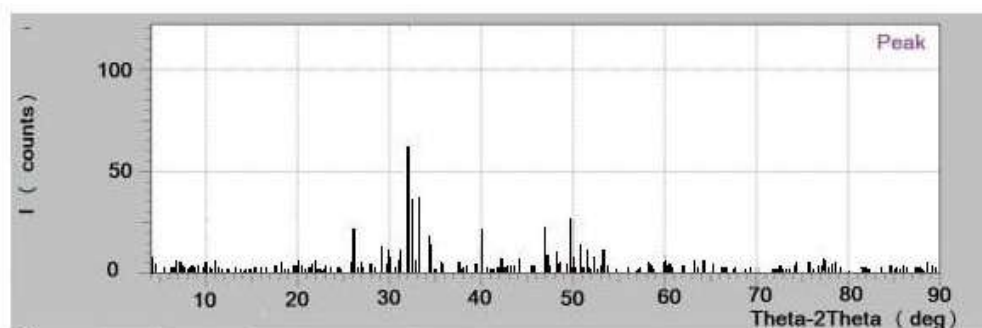


Figure 2. XRD pattern of HANP presenting sharp diffraction peak.

1.3. Functional groups identification by FTIR: The results of FTIR spectra of the prepared HANPs are shown in figure 3.

The spectra indicate the presence of phosphate and hydroxyl groups in hydroxyapatite, the peaks in the broad band around 1000 cm^{-1} and 1100 cm^{-1} shows the presence of PO_4^{3-} group that appear in asymmetric stretching mode of vibration. The characteristic bands for PO_4^{3-} appear also at 470, 568, 602, 964, 1041 and 1093 cm^{-1} . The asymmetric P-O stretching vibration mode of the PO_4^{3-} bands at 964 cm^{-1} is a distinguishable peak, together with the sharp peaks at 633, 602, 568 cm^{-1} correspond to the triply degenerating banding vibrations of PO_4^{3-} in hydroxyapatite, which are characteristics for hydroxyapatite. There is also a sharp peak at 3571 cm^{-1} refers to the stretching vibration of the OH^- ions.

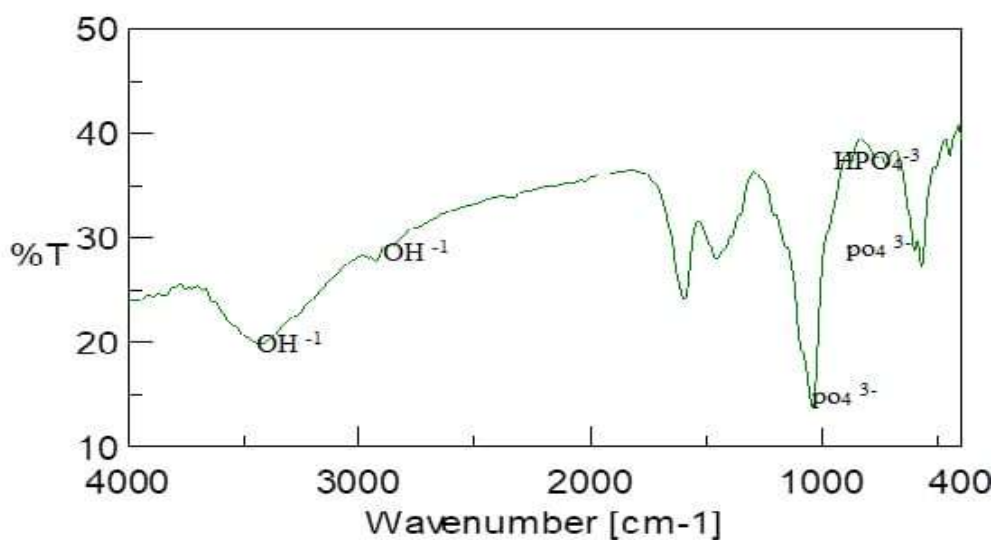


Figure 3. FTIR spectra of the synthesized HANPs.

1.4. Thermal stability and elemental analysis

Figure 4 shows the weight percent in the prepared NHAPs with heating. The range of heating from 50°C to 850°C. A slight decline in the weight loss % was noticed in the range from 50 – 250°C. Also, NHAPs showed 5% weight loss at 600°C. The first derivative of weight loss against temperature shows a peak at 600°C, and no further peaks till 850°C was observed.

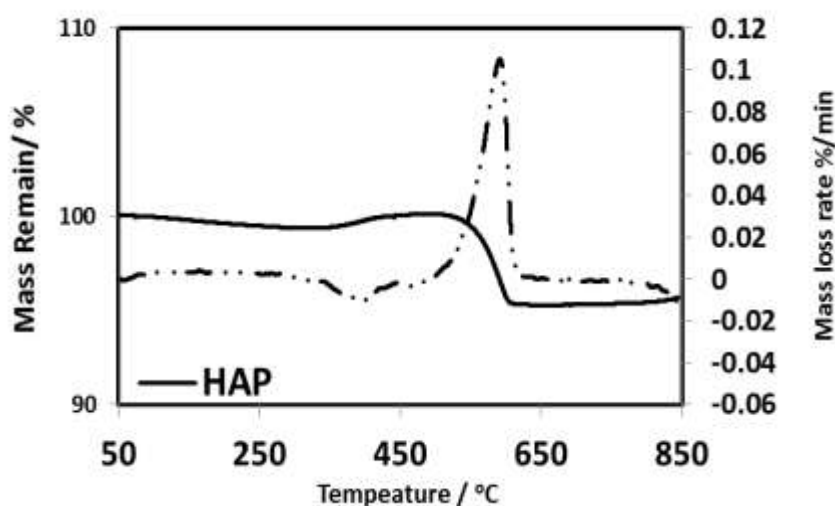


Figure 4. Thermal stability of HANP

2. Effects of BPA and HANPs on liver function parameters

The current findings revealed that liver enzymes; ALT and AST increased significantly in the BPA intoxicating group ($p \leq 0.001$) when compared to the negative control one. On the other hand, these elevations were notably reduced in the treated group, HANPs + BPA. Obviously, there

is no statistically significant difference between the negative control (NC) and HANPs group.

Total protein concentration showed no significant changes in the N.C and HANPs group, while the BPA group had a significant decrease ($p \leq 0.001$) when compared to the control one. Importantly, the treated group (HANPs + BPA) exhibited an enhancement in total protein levels, which offset the effect of BPA exposure.

Accordingly, serum Albumin levels were decreased upon exposure to BPA; in this concern there was no obvious difference between the control, HANPs, and HANPs + BPA groups (Table 1).

Table 1: Effects of BPA and HANPs on liver function parameters.

TEST GROUPS	AST(U/L)	ALT(U/L)	TOTAL PROTEIN(G/D L)	ALBUMIN (G/DL)
Negative Control	130±21.6	30.67±5.0	11.27±0.5	4.23±0.55
HANP	122±15.1	55.33±8.08	11.33±1.09	4.03±0.25
% change	6.1%	80%	0.53%	4.7%
BPA	570±43.26***a	284.67±41.1***a	8.2±0.5***a	3.53 ±0.15**a
% change	338.4 %	828.2%	27.24%	16.5%
HANPs+BPA	343.3±57.7***b	251.0±44.45* ^b	10.73±0.603 *** ^b	4.27±0.15*** ^b
% change	164%	718.3%	4.79%	0.9%

Data are expressed as mean ±SD (n=10), *** $p \leq 0.001$, ** $p \leq 0.01$ when compared to the control group, **^b $p \leq 0.01$, *^b $p \leq 0.05$, ***^b $p \leq 0.001$ as compared to BPA group. The % change was compared to the negative control group.

3. Effects of BPA and HANPs on lipid profile

As shown in table 2, total cholesterol increased significantly ($p \leq 0.001$) in the BPA-intoxicated rats when compared to the negative control group, as did triglycerides, and LDL-Ch ($p \leq 0.01$ and $p \leq 0.05$) respectively. Consistently, HDL-Ch was significantly decreased ($p \leq 0.001$). Fortunately, the treated group (HANPs + BPA) mitigated the toxic effect of BPA exposure, as evidenced by the significant reduction ($P \leq 0.01$, $P \leq 0.05$) in the cholesterol and triglycerides levels, respectively, with significant restoring ($P \leq 0.01$) in the HDL-Ch, as compared to the BPA group. However, no modulation in the LDL-Ch levels was noticed in the treated group, as compared to the BPA one.

Table 2: Effects of ingested BPA and HANPs treatment on lipid profile indicators.

PARAMETER GROUPS (N=10 ANIMALS EACH)	TOTAL CHOLESTEROL (MG/DL)	TRIGLYCE RIDES (MG/DL)	HDL-CH (MG/DL)	LDL-CH (MG/DL)
Negative control	135±12.24	65±3.6	115.33±10.01	14.19±2.5
HANPs	196.67±17.0	80.0±8.7	70.33±12.34	12.72±2.75
BPA	272.57±23.76** *a	77.33±7.0**a	63.33±11.93***a	16.3±3.75*a
HANP+BPA	173.0±39.74**b	69.67±7.09*b	108.33±23.86**b	16.68±2.65

Data are expressed as mean ±SD (n=10). * $p \leq 0.05$ ** $p \leq 0.01$, *** $p \leq 0.001$ compared to the negative control group * $p \leq 0.05$, ** $p \leq 0.01$ compared to the BPA group.

DISCUSSION

This study aimed to construct nanoparticles of hydroxyapatite (HANPs) as a novel formula for efficient removal of BPA and thus modulate its harmful effects in living systems after exposure to BPA. The nano structure of the prepared HANPs showed large surface area that resulted in clusters formation which contain pores and channel that increase adsorption of BPA on HANPs.

The XRD pattern of the constructed nanoparticles revealed peaks at 2 theta positions; 32.04, 33.177 and 32.44, confirming the high crystallinity of the prepared HANPs, and agreeing with the standard XRD pattern of hydroxyapatite from JCPDS (896438) Joint Committee on Powder Diffraction Standards. Moreover, the d-spacing values matched the standard hydroxyapatite and were equal to 2.79Å, 2.69Å and 2.75Å, which are in good agreement with Bouyer *et al.*, (2000), indicating successful crystallinity. Moreover, the results fit the hexagonal structure of hydroxyapatite (JCPDS file number 9-0432). By using Scherrer formula, the size of the prepared hydroxyapatite is calculated as approximately equals to 65 nm.

As known, the chemical formula of HAP is $(Ca)_{10}(PO_4)_6(OH)_2$. The $(PO_4)_6$, and $(OH)_2$ are usually considered as ion-exchangeable groups. These functional groups of the prepared HANPs were in aligned with results obtained from Choi *et al.* (2004), according to the obtained FTIR pattern. As shown in the FTIR pattern of the prepared HANPs, peaks at 3572 cm^{-1} is

corresponding to the OH⁻ groups; peaks in the region from 1960 and 2220 are related to the vibration mode for PO₄⁻³ and consistent with the results of Koutsopoulos, 2002; Silvester, 2013; Diallo-Garcia, 2014. The peak at 470 cm⁻¹ resembles to double-degenerated bending modes of the O–P–O bonds and is aligned with the study of Klee & Engel, 1970. The peak at 1000 cm⁻¹ is attributed to the asymmetric stretching vibrations of the P–O bonds.

The functional PO₄⁻³ group of the prepared HANPs showed peaks at 470, 568, 602 and 633 cm⁻¹ which represents the asymmetric bending vibration mode. These observations are consistent with the results of Destainville, 2003; Mobasherpour & Heshajin, 2007; Mekhemer *et al.*, 2019; Malpica-Maldonado, 2019 who detected the PO₄⁻³ group at peaks 570 and 601 cm⁻¹. Additionally, the ion stretching mode of the OH⁻ functional group that appeared at 3571 cm⁻¹ in our prepared HANPs was aligned with the previous ones which appeared at 632 and 3417 cm⁻¹ (Raynaud, 2002; Destainville, 2003; Malpica-Maldonado, 2019; Mekhemer *et al.*, 2019). The PO₄⁻³ group detected at peaks 1000, 1100, 1041 and 1093 and resemble the asymmetric stretching mode of vibration was in accordance with the previous findings of Raynaud, 2002; Destainville, 2003; Mobasherpour & Heshajin, 2007; Adeogun, 2018; Malpica-Maldonado, 2019) who recorded peaks at 1049, 1095 cm⁻¹.

Thermal analysis of the prepared HANPs using TG revealed 2 different types of water in their structure; the lattice and adsorbed water (Le Geros *et al.*, 1978); the adsorbed water is characterized by its reversibility and thermal instability at temperature from 50 to 250°C. Also, it can be noticed that loss of water occurred without affecting lattice parameters. On the other hand, the lattice water is irreversible lost until heated at temperature 600 °C that lead to a collapse in the lattice dimension. When HANPs were heated at high temperature, dehydration took place by releasing OH⁻ and producing oxyhydroxyapatite (OHAP) (Locardi *et al.*, 1993). Moreover, results from thermal analysis showed the highest thermal stability and the slowest rate of mass loss. The HANPs are thermally stable in the temperature range 25 to 600 °C; Another stable a plateau was reached above 600°C, indicating that OHAP is highly thermal stable at temperatures above 600°C.

In order to evaluate the protective effect of the prepared HANPs against BPA-induced hepatotoxicity in rats, selected serum biochemical parameters were assessed. BPA can cause severe liver dysfunction, injury which was confirmed by the dramatic alterations in liver enzyme levels and lipid profile. On the other hand, HANPs were shown to modulate these parameters and hence mitigated the BPA-inducing hepatotoxicity. Hepatic injury is mainly measured with the use of serum ALT and AST levels. Despite the far specificity of ALT over AST (Nagel *et al.*, 1997) in detecting damaged

hepatocytes, increased levels of both enzymes are considered to be an indicator of hepatic damage.

The current results reveal that there is a significant increase in both ALT and AST levels. These findings are in agreement with those of Praveena *et al.*, 2018; Acaroz *et al.*, 2019; Lee *et al.*, 2019; Soundararajan *et al.*, 2019 who confirmed the hepatotoxic impact of BPA. As well known, increased these liver enzyme levels in serum reflected the tissue injury and hepatic damage (Giannini *et al.*, 2005). These dramatic increments in liver enzymes may be arising from the stimulation of liver activity induced by BPA ingestion (Lozano-Paniagua *et al.*, 2021)

The effect of BPA on the liver function was well confirmed by the significant reduction in the total protein levels in the BPA group, when compared to the negative control group ($P \leq 0.01$) which is in agreement with Verma & Sangai, (2009). This reduction may be due to the deactivation of protein disulfide isomerase, a protein that is involved in the folding and shedding of cellular proteins (Hiroi *et al.*, 2006). BPA induce stress, which causes a decrease in protein, and amino acids used in several catabolic reactions. Moreover, BPA may inhibit or activate various enzymic activities that downregulate the expression of total protein encoding genes (Zhang *et al.*, 2005).

Because the liver was the target organ for toxic compounds *via* conjugation and detoxification, hepatic synthesis of albumin levels decreased significantly in the BPA group (Segre, 1975). BPA and other toxic compounds can significantly reduce protein profile. In line with, Hanioka *et al.*, 1998 reported that BPA promote a significant reduction in liver serum proteins in rats.

In this study, BPA group had a significant increase in cholesterol levels, indicating its ability to cause accumulation of fat droplets in cells. These findings are consistent with the previous studies indicating that long-term exposure to BPA causes an increase in cholesterol levels (Marmugi *et al.*, 2014; Lin *et al.*, 2017). Dyslipidemia and accumulation of TG and cholesterol in liver was associated with the increased levels of triglycerides, LDL-Ch with concomitant reduction in the HDL-Ch levels in BPA groups. These results are aligned with Lin *et al.* (2017), who found that BPA exposure altered the fatty acids pattern as well as the gene responsible for lipogenesis and cholesterol synthesis. In addition, BPA exposure increases hepatic lipid accumulation as a result of increased expression of the transcription factor and sterol regulatory binding protein-1 that activates enzymes of lipogenesis and lipid accumulation in liver (Marmugi *et al.*, 2012).

On the other hand, ingestion of HANPs along with BPA administration in the treated group of rats was shown to alleviate the toxic effects of BPA. Actually, when HANPs were taken orally, it reaches the stomach and

dissolved by gastric acid releasing calcium and phosphate ions (Margolis & Moreno, 1992). Calcium plays a very important and protective role to liver by inhibiting lipid accumulation (Kakimoto & Kowaltowski, 2016) as calcium can bind to fatty acids in colon and inhibit its absorption (Soares & She-Ping-Delfos, 2010). HANP+BPA group modulates the detected alterations in liver enzymes; ALT and AST as calcium can protect liver from oxidative stress that appears in BPA group which change the hepatic metabolism. As well as calcium can prevent the increase in lipid profile levels which is similar to results founded by Shifdar *et al.* (2020) who proved the effect of calcium on decreasing risk of cardiovascular diseases by lowering serum levels of cholesterol.

Consistently, HANPs were proved as being biosafe and had no side effect on vital organs as kidney and liver as confirmed by Aoki *et al.* (2000) that reported the intravenous injection of HANPs to dogs with a dose of 26 mg/kg for 2 weeks intervals among two years and Wang *et al.*, (2012) proved that serum levels of ALT, AST, blood urea and creatinine were not affected or changed when rats were injected intraperitoneally with HANPs (8.3 mg/ml) 3 times/ week for 4 consecutive weeks.

Based on the results of this study, it can be concluded that the HANPs chemically synthesized by sol-gel method with 65 nm in size, can be orally used safely by at a concentration of 1g / kg/ bwt. This ingested concentration has the ability to eliminate the toxic effects resulted from the exposure to

BPA. There was no significant fluctuation in the levels of lipid profile and liver enzymes when compared to the negative control group. Hence, it can be decided that HANPs were found to be nontoxic to rats at the cellular level under the aforementioned laboratory conditions. Further studies are needed to study the effect of administrating 10% DMSO on renal function parameters in normal animals.

REFERENCES

- Acaroz, U.; Ince, S.; Arslan-Acaroz, D.; Gurler, Z.; Demirel, H.H.; Kucukkurt, I.; Eryavuz, A.; Kara, R.; Varol, N. & Zhu, K. (2019). Bisphenol-A induced oxidative stress, inflammatory gene expression, and metabolic and histopathological changes in male Wistar albino rats: protective role of boron. *Toxicol. Res. (Camb.)*, 8 (2): 262–269.
- Adeogun, A.I.; Ofudje, A.E.; Idowu, M.A. & Kareem, S.O. (2018). Facile development of nano size calcium hydroxyapatite based ceramic from eggshells: synthesis and characterization. *Waste and Biomass Valorization*, 9 (8): 1469-1473.
- Allain, C.C.; Poon, L.S., Chan, Richmond, W. & Fu, P.C. (1974). Enzymatic Determination of Total Serum Cholesterol. *Clinical chemistry*, 20 (4): 470-475. <https://doi.org/10.1093/clinchem>
- Alonso-Magdalena, P.; Morimoto, C.; Ripoll, E.; Fuentes & Nadal, A. (2006). The estrogenic effect of bisphenolA disrupts the pancreatic β -cell function *in vivo* and induces insulin resistance. *Environ. Health Perspect*, 114: 106-112.
- Aoki, H.; Kutsuno, T.; Li, W. & Niwa, M. (2000). An *in vivo* study on the reaction of hydroxyapatite-sol injected into blood. *J. Mater. Sci. Mater. Med.*, 11: 67–70.

- Bindhumol, V.; Chitra, K.C. & Mathur, P.P. (2003). Bisphenol A induces reactive oxygen species generation in the liver of male rats. *Toxicology*, 188: 117–124.
- Bouyer, E.; Gitzhofer, F. & Boulos, M.I. (2000). Morphological study of hydroxyapatite nanocrystal suspension. *J. Mater. Sci. Mater Med*, 11: 523-531.
- Braga, O.; Smythe, G.A.; Schäfer, A. & Feitz, A.J. (2005). Steroid Estrogens in Primary and Tertiary Wastewater Treatment Plants. *Water Science & Technology*, 52 (8): 273-278.
- Chitra, K.C.; Latchoumycandane, C. & Mathur, P.P. (2003). Induction of oxidative stress by bisphenol A in the epididymal sperm of rats. *Toxicology*, 185: 119–127.
- Choi, D.; Marra, K. & Kumta, P.N. (2004). Chemical synthesis of hydroxyapatite/poly (caprolactone) composite. *Materials Research Bulletin*, 39: 417-432
- Corrales, J.; Kristofco, L.A.; Steele, W.B.; Yates, B.S.; Breed, C.S.; Williams, E.S. & Brooks, B.W. (2015). Global assessment of bisphenol A in the environment: Review and analysis of its occurrence and bioaccumulation. *Dose Response*, 13(3): 1559325815598308 doi:10.1177/1559325815598308
- Descamps, M., Hornez, J.C. & Leriche, A (2009). Manufacture of Hydroxyapatite Beads for Medical Applications, *Journal of the European Ceramic Society*, 29: 369-375 <https://doi.org/10.1016/j.jeurceramsoc.2008.06.008>.
- Destainville, A.; Champion, E.; Bernache-Assollant, D. & Laborde, E. (2003). Synthesis, characterization and thermal behavior of apatitic tricalcium phosphate, *Mater. Chem. Phys.* 80 (1): 269-277.
- Diallo-Garcia, S.; Ben Osman, M.; Krafft, J.M.; Casale, S.; Thomas, C.; Kubo, J.G. & Costentin, J. (2014). *Phys. Chem. C*, 118: 12744-12757.

- Dorozhkin, S.V. (2012). Calcium Orthophosphates: Applications in Nature, Biology, and Medicine; CRC Press: Boca Raton, FL, USA, ISBN 978-981-4364-1
- Fan, Z.; Hu, J.; An, W. & Yang, M. (2013). Detection and occurrence of chlorinated byproducts of bisphenol A, nonylphenol, and estrogens in drinking water of china: comparison to the parent compounds. *Environ Sci Technol*, 47:10841–10850. <https://doi.org/10.1021/es401504a>.
- Fathi, M. H., Hanifi, A. & Mortazavi, V. (2008). The occurrence and risk assessment of phenolic endocrine-disrupting chemicals in Egypt's drinking and source water. *Journal of Materials Processing Technology*, 202 (1–3): 536-542.
- Fihri, A.; Len, C.; Varma, R.S & Solhy, A. (2017). Hydroxyapatite: A review of syntheses, structure and applications in heterogeneous catalysis. *Coordination Chemistry Reviews*. 347: 48-76.
- Finley, P.R.; Schiffman, R.B., Williams R.J. & Lichti, D.A. (1978). Cholesterol in high-density lipoprotein: Use of mg²⁺/dextran sulfate in its enzymic measurement. *Clinical chemistry*, 24(6): 931-933.
- Fossati, P. & Prencipe, L. (1982). Serum Triglycerides Determination Colorimetrically with an Enzyme That Produces Hydrogen Peroxide. *Clinical Chemistry*, 28: 2077-2080.
- Giannini, E.G.; Testa, R. & Savarino, V. (2005). Liver enzyme alteration: a guide for clinicians. *Canadian Med Associat J*, 172: 367–379.
- Gupta, K.; Bhattacharya, S.; Chattopadhyay, D.J.; Mukhopadhyay, A.; Biswas, H.; Dutta, J.; Roy, N.R. & Ghosh, U.C. (2011). Ceria associated manganese oxide nanoparticles: Synthesis, characterization and arsenic (V) sorption behavior. *Chemical Engineering Journal*, 172: 219- 229.
- Hanioka, N.; Jinno, H.; Nishimura, T. & Ando, M. (1998). Suppression of male-specific cytochrome p 450 isoforms by Bisphenol-A in rat liver. *Archives of Toxicology*, 72(7): 387-394.

- Hanioka, N.; Naito, T. & Narimatsu, S. (2008). Human UDP-glucuronosyltransferase isoforms involved in bisphenol A glucuronidation. *Chemosphere*, 74(1): 33-36. <https://doi.org/10.1016/j.chemosphere.2008.09.053>.
- Hernandez-Rodriguez, G.; Zumbado, M.; Luzardo, O.P.; Monterde, J.G.; Blanco, A. & Boada, L.D. (2007). Multigenerational study of the hepatic effects exerted by the consumption of Haniokanonylphenol and 4-octylphenol contaminated drinking water in Sprague- Dawley rats. *Environ. Toxicol. Pharmacol*, 23: 73-81.
- Hiroi, T.; Okada, K.; Imaoka, S.; Osada, M. & Funae, Y. (2006). Bisphenol A binds to protein disulfide isomerase and inhibits its enzymatic and hormone binding activities. *Endocrinology*, 147 (6): 2773 – 2780.
- Hsieh, M.; Perng, L.; Chin, T. & Perng, H. (2001). Phase purity of sol-gel-derived hydroxyapatite ceramic. *Biomaterials*, 22(19): 2601-2607.
- Kabuto, H.; Amakawa, M. & Shishibori, T. (2004). Exposure to bisphenol A during embryonic/fetal life and infancy increases oxidative injury and causes underdevelopment of the brain and testis in mice. *Life Sci*, 74: 2931–2940.
- Kakimoto, P.A. & Kowaltowski, A.J. (2016). Effects of high fat diets on rodent liver bioenergetics and oxidative imbalance. *Redox Biology*, 8: 216-225
- Klee, W.E. & Engel, G. (1970). Infrared spectra of the phosphate ions in various apatites. *J Inorg Nucl Chem*, 32: 1837–1843
- Kopf, M.; Bachmann, M.F. & Marsland, B.J. (2010). Averting inflammation by targeting the cytokine environment. *Nature reviews. Drug Discovery*, 9: 703-718.
- Kuhn, R. (2022). Environmental Nanotechnologies in Wastewater Treatment. In *Encyclopedia*. <https://encyclopedia.pub/entry/21060>
- Lang, I.A.; Galloway, T.S.; Scarlett, A.; Henley, W.E.; Depledge, M.; Wallace, R.B. & Melzer, D. (2008). Association of urinary

- bisphenol A concentration with medical disorders and laboratory abnormalities in adults. *JAMA*, 300: 1303–1310.
- Lee, J.; Hong, S.; Sun, J.H.; Moon, J.K.; Boo, K.H. ; Lee, S.M. & Lee, J.W. (2019) .Toxicity of dietary selenomethionine in juvenile steelhead trout, *Oncorhynchus mykiss*: tissue burden, growth performance, body composition, hematological parameters, and liver histopathology, *Chemosphere*,226: 755–765.
- LeGeros, RZ.; Bonel, G. and Legros, R. (1978). Types of H₂O in human enamel and in precipitated apatites. *Calcif Tiss Res*. 26: 111-118.
- Lin ,Y.; Ding, D.; Huang, Q.; Liu, Q.; Lu, H.; Lu, Y.; Chi, Y.; Sun, X.; Ye ,G.; Zhu, H. (2017) Downregulation of miR-192 Causes Hepatic Steatosis and Lipid Accumulation by Inducing SREBF1: Novel mechanism for bisphenol A-triggered non-alcoholic fatty liver disease. *Biochim Biophys Acta Mol Cell Biol Lipids*. 1862: 869–882.
- Lindholst, C.; Wynne ,P.M.; Marriott ,P.; Pedersen ,S.N. & Bjerregaard,P. (2003) .Metabolism of bisphenol a in zebrafish (*Danio rerio*) and rainbow trout (*Oncorhynchus mykiss*) in relation to estrogenic response. *Comp Biochem Physiol Toxicol Pharmacol*, 135(2): 169-177.
- Locardi, B.; Pazzaglia, U.E.; Gabbi, C. & Pro"lo, B. (1993). Thermal behaviour of hydroxyapatite intended for medical applications. *Biomaterials.*, 14: 437-441.
- Lowry, O.H.; Rosebrough, N.J.; Farr, A.L. & Randall, R.J. (1951). Protein measurement with folin phenol reagent. *The journal of biological chemistry*, 193: 265-275.
- Lozano-Paniagua, D.; Parron, T.; Alarcon, R.; Requena, M.; Lopez-Guarnido, O.; Lacasana, M .& Hernandez, A.F. (2021). Evaluation of conventional and non-conventional biomarkers of liver toxicity in greenhouse workers occupationally exposed to pesticides.

- Mahabole, M.P.; Aiyer, R.C.; Ramakrishna, C.V.; Sreedhar, B. & Khairnar, R.S. (2005). Synthesis, characterization and gas sensing property of hydroxyapatite ceramic". *Bull. Mater. Sci*, 28 (6): 535–545.
- Malpica-Maldonado, J.J.; Melo-Banda, J.A.; Martínez-Salazar, A.L. & Garcia-Hernandez, M. (2019). Synthesis and characterization of NiMo₂C particles supported over hydroxyapatite for potential application as a catalyst for hydrogen production, *Int. J. Hydrogen Energy*, 44 (24): 12446-12454.
- Margolis, H.C. & Moreno, E.C. (1992). Kinetics of hydroxyapatite dissolution in acetic, lactic, and phosphoric acid solutions. *Calcified Tissue International* 50 (2): 137-143. doi: 10.1007/BF00298791.
- Marmugi, A.; Ducheix, S.; Lasserre, F.; Polizzi, A.; Paris A, Priymenko, N.; Bertrand-Michel, J.; Pineau, T.; Guillou, H.; Martin. P.G. & Mselli-Lakhal, L. (2012). Low doses of bisphenol A induce gene expression related to lipid synthesis and trigger triglyceride accumulation in adult mouse liver. *Hepatology*, 55: 395–407.
- Marmugi, A., Lasserre, F., Beuzelin, D., Ducheix, S., Huc, L., Polizzi, A., Chetivaux, M., Pineau, T., Martin, P., Guillou, H. & Mselli-Lakhal, L. (2014). Adverse effects of long-term exposure to bisphenol A during adulthood leading to hyperglycaemia and hypercholesterolemia in mice. *Toxicology*. 325: 133-143. doi: 10.1016/j.tox.2014.08.006.
- Mekhemer, G.A.; Bongard, H.; Shahin, A.A. & Zaki, M.I. (2019). FTIR and electron microscopy observed consequences of HCl and CO₂ interfacial interactions with synthetic and biological apatites: influence of hydroxyapatite maturity, *Mater. Chem. Phys*, 221: 332-341.
- Michalowicz, J. (2014). Bisphenol-A-Sources, toxicity and biotransformation. *Environ. Toxicol. Pharmacol*, 37: 738-758.

- Mobasherpour, I. & Heshajin, M. (2007). Synthesis of nanocrystalline hydroxyapatite by using precipitation method, *J. Alloy. Comp*, 430: 330-333.
- Moon, M.K.; Kim, M.J.; Jung, I.K.; Koo, Y.D.; Ann, H.Y.; Lee, K.J.; Kim, S.H.; Yoon, Y.C.; Cho, B.J.; Park, K.S.; Jang, H.C. & Park, Y.J. (2012). Bisphenol A impairs mitochondrial function in the liver at doses below the no observed adverse effect level. *Journal of Korean Medical Science*, 27: 644-652.
- Mourad, I.M. & Khadrawy, Y.A. (2012). The sensitivity of liver, kidney and testis of rats to oxidative stress induced by different doses of bisphenol A. *Life*, 50:19.
- Nagel, S.C.; Vom Saal, F.S.; Thayer, K.A.; Dhar, M.G.; Boehler, M. & Welshons, W.V. (1997). Relative binding affinity-serum modified access (RBA-SMA) assay predicts the relative in vivo bioactivity of the xenoestrogens bisphenol A and octylphenol. *Environ Health Perspect*, 105L: 70–76.
- Noureddine, El. S.; Moussawi, R.; Karam, M.; Cladiere, H.; Chebib, R.; Ouaini, V. & Camel, (2018). Effect of sterilisation and storage conditions on the migration of bisphenol A from tinplate cans of the Lebanese market, *Food Addit. Contam. Part A Chem. Anal. Control Expo. Risk Assess*, 35 (2): 377–386.
- Petteri, N. (2002). Effects of bisphenol-A and phytosterols on the European polecat (*Mustelaputorius*) and the field vole (*Microtusagrestis*). Academic Dissertation, Department of Medicine, University of Helsinki for public examination in Auditorium, ISBN 952-91-4484-9 (Print). ISBN 952-10-0533-5.
- Prakasam, M.; Locs, J.; Salma-Ancane, K.; Loca, D.; Largeteau, A. & Berzina-Cimdina, L. (2015). Fabrication, properties and applications of dense hydroxyapatite: A review. *J. Funct. Biomater.* 6: 1099–1140.

- Praveena, S.M.; Teh, S.W.; Rajendran, R.K.; Kannan, N.; Lin, C.C.; Abdullah, R. & Kumar, S. (2018). Recent updates on phthalate exposure and human health: a special focus on liver toxicity and stem cell regeneration, *Environ. Sci. Pollut. Res. Int*, 25 (12): 11333–11342.
- Radwan, E.K.; Ibrahim, M.B.M.; Adel, A. & Farouk, M. (2020). The occurrence and risk assessment of phenolic endocrine-disrupting chemicals in Egypt's drinking and source water. *Environ Sci Pollut Res Int*, 27(2): 1776-1788. doi: 10.1007/s11356-019-06887-0. Epub 2019 Nov 22. PMID: 31758477.
- Raynaud, S.; Champion, E.; Bernache-Assollant, D. & Thomas, P. (2002). Calcium phosphate apatites with variable Ca/P atomic ratio I. Synthesis, characterisation and thermal stability of powders, *Biomaterials*, 23 (4): 1065-1072.
- Reitman, S. & Frankel, S. (1957). Colorimetric method for the determination of serum glutamic – oxaloacetic and glutamic- pyruvic transaminases. *Am. J. clin*, 28: 56-63.
- Rochester, J.R. (2013). Bisphenol A and human health: a review of the literature. *Reprod Toxicol*, 42:132-155. <https://doi.org/10.1016/j.reprotox.2013.08.008>.
- Rubin, B.S. (2011). Bisphenol-A: An endocrine disruptor with widespread exposure and multiple effects. *J. Steroid. Biochem*, 127: 27– 34.
- Segre, E.J. (1975). Naproxen metabolism in man. *J. Clin. pharmacol*, 15, 316.
- Shidfar, F.; Moghayedi, M.; Kerman, S.R.J.; Hosseini, S. & Shidfar, S. (2010). Effects of a calcium supplement on serum lipoproteins, apolipoprotein B, and blood pressure in overweight men *Int J Endocrinol Metab*, 8 (4): 194-200.
- Silvester, L. (2013). Synthesis of higher alcohols from ethanol over hydroxyapatite-based catalysts, Lille University.

- Soares, M.J. & She-Ping-Delfos, W.L.C. (2010). Postprandial energy metabolism in the regulation of body weight: is there a mechanistic role for dietary calcium? *Nutrients*, 2: 586-598
- Soundararajan, A.; Prabu, P.; Mohan, V.; Gibert, Y. & Balasubramanyam, M. (2019). Novel insights of elevated systemic levels of bisphenol-A (BPA) linked to poor glycemic control, accelerated cellular senescence and insulin resistance in patients with type 2 diabetes, *Mol. Cell. Biochem*, 458:171-183.
- Surmenev, R.A.; Surmeneva, M.A. & Ivanova, A.A. (2014). Significance of calcium phosphate coatings for the enhancement of new bone osteogenesis—a review. *Acta Biomater.* 10: 557–579.
- Verma, R.J. & Sangai, N.P. (2009). The ameliorative effect of black tea extract and quercetin on bisphenol A induced cytotoxicity. *Acta Poloniae Pharmaceutica*, 66: 41-44.
- Wang, L.; Zhou, G.; Liu, H.; Niu, X.; Han, J.; Zheng, L. & Fan, Y. (2012). Nano-hydroxyapatite particles induce apoptosis on MC3T3-E1 cells and tissue cells in SD rats. *Nanoscale*, 4: 2894–2899.
- Wu, J.B.; Chuang, H.R.; Yang, L.C. & Lin, W. C. (2010). A standardized aqueous extract of *Anoectochilus formosanus* ameliorated thioacetamide-induced liver fibrosis in mice: The role of Kupffer cells. *Bioscience, Biotechnology, and Biochemistry*, 74: 781 – 787.
- Xu, W.; Yan, W.; Huang, W.; Miao, L. & Zhong, L. (2014). Endocrine-disrupting chemicals in the Pearl River Delta and coastal environment: sources, transfer, and implications. *Environ Geochem Health*, 36(6): 1095- 1104. <https://doi.org/10.1007/s10653-014-9618-3>.
- Ye, B.S.; Leung, A.O.W. & Wong, M.H. (2017). The association of environmental toxicants and autism spectrum disorders in children. *Environ. Pollut*, 227: 234–242.

Zhang, G.X.; Kimura,S.; Nishiyama, A.; Shokoji, T.; Rahman, M.; Yao, L.; Nagai, Y.; Fujisawa, Y.; Miyatake, A. & Abe, Y.(2005). Cardiac oxidative stress in acute and chronic isoproterenol-infused rats. *Cardiovasc Res*, 65(1): 230-238.

تخفيف المشكلات الصحية الضارة الناتجة عن التعرض لثنائي الفينول أ باستخدام نانو هيدروكسي أباتيت

سارة محمود إبراهيم^(١) - محمد مختار^(٢) - هالة مهدى الدسوقي^(٣) - جبرمين محسن حمدي^(٣)
(١) قسم العلوم البيئية الأساسية كلية الدراسات العليا والبحوث البيئية، جامعة عين شمس (٢) الكلية
الهندسة الكيميائية. مصر كلية العلوم - جامعة عين شمس قسم الكيمياء
الحيوية- مصر

المستخلص

يعتبر ثنائي الفينول أ (BPA) من أخطر الملوثات البيئية. بمجرد دخوله للجسم يتم التخلص منه بواسطة الكبد وبالتالي يتسبب في إصابة الكبد بالعديد من الامراض. تم اختيار مركب نانو هيدروكسي أباتيت (HANP) في الدراسة الحالية كطريقة آمنة لامتصاص مادة ثنائي الفينول أ وبالتالي تجنب آثارها السامة في الجسم.

تم تحضير مركب نانو هيدروكسي أباتيت بواسطة تقنيات sol-gel ، وتم توصيفه بواسطة XRD. أجريت دراسة على أربعين من ذكور جرذان تم تقسيمها عشوائيا إلى ٤ مجموعات (١٠ فئران/مجموعة). تلقت المجموعة الضابطة ١٠٪ من محلول DMSO ، ومجموعة نانو هيدروكسي أباتيت ١ جم HANP / كجم / وزن / يوم، ومجموعة ثنائي الفينول أ 100 مجم BPA / كجم / وزن / يوم والمجموعة المعالجة اخذت (BPA + HANP) ١ جم / HANP ١٠٠ مجم BPA / كجم وزن / يوم. أعطيت الجرعات يوميا لمدة ستة أسابيع متتالية عن طريق الفم. تم جمع عينات الدم وفصل المصل لقياس إنزيمات الكبد المختارة و مجموعة الدهون الكاملة بالدم.

زادت مستويات انزيمات الكبد (ALT و AST) بشكل ملحوظ مع انخفاض مستويات البروتين الكلي والألبومين في مجموعة ثنائي الفينول أ مقارنة بالمجموعة الضابطة. كما زادت مستويات الكوليسترول والدهون الثلاثية ونقص في مستوى الكوليسترول المرتبط بالدهون عالية الكثافة في

مجموعة ثنائي الفينول أ . أظهرت المجموعة المعالجة تحسناً كبيراً في جميع القياسات مقارنة بمجموعة ثنائي الفينول أ .
في الختام، تعتبر نانو هيدروكسي ابنتيت مادة حيوية فعالة يمكنها تقليل الاثار الضارة للكبد الناتجة عن التعرض لملوث ثنائي الفينول أ .
الكلمات الدالة: ثنائي الفينول أ، مشاكل صحية، إنزيمات الكبد، صورة الدهون، جزيئات النانو هيدروكسي أبنتيت.